International Journal of Control and Automation
Vol. 10, No. 2 (2017), pp.147-160
http//dx.doi.org/10.14257/ijca.2017.10.2.13

Suppression Control for Joint Impact Torque caused by Joint-Locked Failure of Space Manipulator under External Force

Tong Li*, Qingxuan Jia, Gang Chen, Hanxu Sun and Bonan Yuan

School of Automation, Beijing University of Posts and Telecommunications, Beijing 100876, China
bupt.litong@gmail.com

Abstract

Aiming at reducing the impact torque caused by joint-locked failure during on-orbit operations of space manipulator, a control method which can guarantee the external force requirement and suppressing joint impact torque simultaneously is proposed. In order to describe the characteristics of impact torque, a dynamics model is established when external force acting on the end-effector. Then boundary conditions for impact torque suppression are analyzed, and a control method is proposed based on torque compensation function, which is constructed with dynamics manipulability and can be applied to achieve global joint torque compensation during the entire operation. Afterwards, diagonal matrix coefficient which represents the degree of compensation is adjusted to achieve impact torque minimal for each joint. Simulation experiments are implemented to verify the effectiveness of the proposed method when constant external force and variable external force act on the end-effector, respectively. Further, rated torque is considered to make the joint torque compensation reasonable.

Keywords*: Space manipulator; Impact torque; Joint-locked failure; Suppression control; External force*

1. Introduction

With the development of space exploration, space manipulator [1, 2] plays more and more important role in space station service, solar wing adjustment, orbiter docking and astronauts walking assistant [3]. During these operations, external force acts on the end-effector of space manipulator. Once joint-locked failure occurs [4], impact torque may occur in joint space and operations space simultaneously, which will bring about damage to manipulator structure and manipulating objects. For purpose of operation completion, the external force acting on the end-effector should be maintained. And in order to decrease the damage on manipulator structure, the joint impact torque should be suppressed. Thus, a control method which can suppress joint impact torque and guarantee external force requirement simultaneously is of great significance for stable and safe operation of space manipulator on orbit.

Currently, researches are concentrated on impact torque of manipulator caused during contact and collision [5, 6], while researches on impact force caused by joint-locked failure are less. Nenchev [7] analyzed the impact dynamics of force impulse at the end-effector of a free-floating space robot, and proposed a control method to make the base and manipulator stable depending on reaction null space. Chung [8] proposed an algorithm based on null space of manipulator dynamics, with which collision impact was reduced and torque requirement of task was guaranteed. Wei [9] analyzed the impact force caused by contact and collision of mobile robot to achieve stable walking. Actually, impact torque caused by joint-locked failure is generated by the shutdown of joint motor because of joint-locked, and has knock-on effect on healthy joint and the end-

ISSN: 2005-4297 IJCA

effector. The dynamics characteristics are quite different from collision impact and contact impact. Thus the dynamics characteristics of impact torque caused by joint-locked failure should be analyzed preferentially, based on which a proper control method should be devoted.

On the other hand, impact torque caused by joint-locked failure behaves as a kind of parameter jumps, which are often involved in fault tolerant research. However, velocity jumps [10, 11] are often concentrated on, while torque jumps are researched less. Typically, Abdi [12] guaranteed the force acting at the end-effector of manipulator via using the characteristics of redundancy. The joint torque was adjusted after joint failure occurred. Unfortunately, the joint torque changed sharply. Besides, the torque jumps caused by joint failure during human robot cooperation was analyzed in another paper [13]. By adjusting the proportion of forces from human and robot, the cooperation force was remained unchanged. In the research above, the torque jumps at the end-effector is concentrated, torque control is not implemented until joint failure occurs. As a result, the reduction for the force jumps at the end-effector may bring about sharp changes in joint torque, which will greatly damage the healthy joints and lead to unsafety in operations. Meanwhile, considering the characteristics of operations on orbit, it is unpractical to achieve impact torque suppression via human cooperation. Thus self-motion ability of space manipulator should be depended on to suppress the impact torque caused by joint-locked failure. And compensation for joint torque should be implemented during the entire operation to avoid the sharp changes.

In conclusion, aiming at guaranteeing external force requirement during on-orbit operation and suppressing the joint impact torque simultaneously, the paper proposed a control method based on global joint torque compensation during the entire operation via self-motion of space manipulator. The paper is formed as follow: The failure condition of space manipulator and the related parameters are list in section 2. A dynamics model of joint impact torque caused by joint-locked failure is established in section 3. The suppression control method is detailed derived in section 4. And simulation experiments are carried out in section 5.

2. Research Object and Related Parameters

The configuration of space manipulator applied on the space station is shown in Figure 1, which consists of the base (space station) and n links. When joint-locked failure occurs, the failure joint loses its motion ability, while other healthy joints can move flexibly. In Figure 1, Configuration A represents the configuration of space manipulator at healthy state, while Configuration B represents the configuration at failure state when the 2nd joint fails. The angle of joint 2 will remain unchanged after joint failure, namely $\theta_2^A = \theta_2^B$ shown in the figure. Correspondingly, the variables related to space manipulator motion are listed as follow:

$\Sigma_I, \Sigma_0, \Sigma_E$ The inertial, base, and terminate frame

Jnt_i The i^{th} joint of space manipulator

c_i The centroid of the i^{th} links

a_i The vector between Jnt_i and c_i

b_i The vector between c_i and Jnt_{i+1}

z_i The direction vector of the i^{th} joint axis

${}^j p_i$ The position vector of joint i related to the j^{th} coordinate system

r_{ci} The position vector of centroid of link i related to the base frame

$v_i, \dot{v}_i$ The linear velocity and acceleration at joint i of space manipulator

$\omega_i, \dot{\omega}_i$ The angular velocity and acceleration of joint i of space manipulator

${}_{i-1}^{i}R$ The rotation transformation from $(i-1)^{th}$ to i^{th} frame

$\theta_i, \dot{\theta}_i, \ddot{\theta}_i$ The i^{th} angel, joint velocity and joint acceleration

m_i, I_i The mass and inertia matrix of link i

f_i, n_i Force and torque at joint i

f_{ci}, n_{ci} Force and torque at the centroid of the i^{th} link

$\boldsymbol{F}_e$ the external force

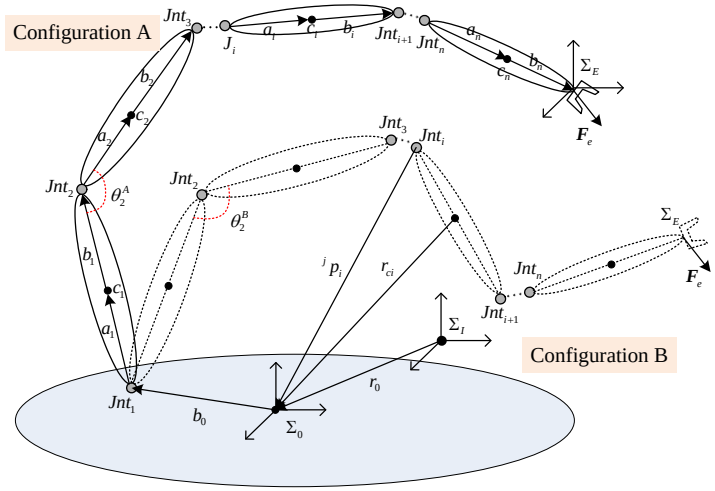

Figure 1. Configuration of Space Manipulator at Healthy and Failure State

3. Dynamic Modeling for Joint Impact Torque

The impact torque caused by joint-locked failure of space manipulator is generated in two aspects: one is the loss of joint driving torque because of motor shutdown, the other one is inertia force caused by velocity variation after joint-locked. And impact torque does not only exist in failure joint, the adjacent joints are affected according to the rigid body dynamics. In this section, since impact torque will bring about changes into dynamics characteristics of each joint, the dynamics model of impact torque is analyzed.

Assume joint-locked failure occurs in joint k at time t_f, the angle will remain unchanged and the joint velocity and acceleration become 0. Then the deviation between time t_f and $t_f + \Delta t$ can be obtained in Equation(1), where Δt means the control cycle in operation.

$$\Delta\theta_k = 0, \Delta\dot{\theta}_k = \dot{\theta}_k^{t_f}, \Delta\ddot{\theta}_k = \ddot{\theta}_k^{t_f} \tag{1}$$

Wherein, $\dot{\theta}_k^{t_f}$, $\ddot{\theta}_k^{t_f}$ represent the value of k^{th} joint velocity and acceleration at time t_f. Affected by the failure, deviations of angular velocity and acceleration at joint k is generated, which can be expressed as Equation (2) with respect to the inertial frame.

$$\begin{aligned} \Delta\omega_k &= \dot{\theta}_k^{t_f} z_k \\ \Delta\dot{\omega}_k &= {}_{k-1}^{k}R\omega_{k-1} \times \dot{\theta}_k^{t_f} z_k + \ddot{\theta}_k^{t_f} z_k \end{aligned} \tag{2}$$

According to Newton-Euler equations, velocity and acceleration at joint 1~joint $k-1$ is not affected by failure joint, while deviations exist in velocity and

acceleration at joint k~joint n. Then for an arbitrary joint i, the angular velocity deviation caused by joint-locked failure can be expressed as:

$$\Delta\omega_i = \begin{cases} 0 & i \in [1, k-1] \\ \dot{\theta}_i^{t_f} z_i & i = k \\ {}_{i-1}^{i}R \cdot \Delta\omega_{i-1} & i \in [k+1, n] \end{cases} \tag{3}$$

Similarly, the angular acceleration deviation at joint i can be expressed:

$$\Delta\dot{\omega}_i = \begin{cases} 0 & i \in [1, k-1] \\ {}_{i-1}^{i}R\omega_{i-1} \times \dot{\theta}_i^{t_f} z_i + \ddot{\theta}_i^{t_f} z_i & i = k \\ {}_{i-1}^{i}R \cdot \Delta\dot{\omega}_{i-1} + {}_{i-1}^{i}R \cdot \Delta\omega_{i-1} \times \dot{\theta}_i^{t_f} z_i & i \in [k+1, n] \end{cases} \tag{4}$$

Besides, it may cause deviations in linear velocity and acceleration because of joint-locked failure, which are influenced by the changes in angular velocity and acceleration. The expression are shown in Equation (5) and (6).

$$\Delta v_i = \begin{cases} 0 & i \in [1, k] \\ {}_{i-1}^{i}R \cdot \Delta\omega_{i-1} \times {}^{i-1}p_i & i = k+1 \\ {}_{i-1}^{i}R(\Delta v_{i-1} + \Delta\omega_{i-1} \times {}^{i-1}p_i) & i \in [k+2, n] \end{cases} \tag{5}$$

$$\Delta\dot{v}_i = \begin{cases} 0 & i \in [1, k] \\ {}_{i-1}^{i}R(\Delta\dot{\omega}_i \times {}^{i-1}p_i + \omega_{i-1} \times (\Delta\omega_{i-1} \times {}^{i-1}p_i) + \\ \Delta\omega_{i-1} \times (\omega_{i-1} \times {}^{i-1}p_i) - \Delta\omega_{i-1} \times (\Delta\omega_{i-1} \times {}^{i-1}p_i)) & i = k+1 \\ {}_{i-1}^{i}R(\Delta\dot{v}_{i-1} + \Delta\dot{\omega}_{i-1} \times {}^{i-1}p_i + \omega_{i-1} \times (\Delta\omega_{i-1} \times {}^{i-1}p_i) + \\ \Delta\omega_{i-1} \times (\omega_{i-1} \times {}^{i-1}p_i) - \Delta\omega_{i-1} \times (\Delta\omega_{i-1} \times {}^{i-1}p_i)) & i \in [k+2, n] \end{cases} \tag{6}$$

Based on the analysis above, for an arbitrary link i, the deviations in force and torque caused by the joint locked failure at the centroid can be represented as:

$$\begin{aligned} \Delta f_{ci} &= m_i \cdot \Delta\dot{v}_i \\ \Delta n_{ci} &= I_i(\Delta\dot{\omega}_i) + \omega_i \times (I_i\Delta\omega_i) + \Delta\omega_i \times (I_i\omega_i) - \Delta\omega_i \times (I_i\Delta\omega_i) \end{aligned} \tag{7}$$

Since the force and torque is derived from the end-effector of space manipulator, then the deviations of force and torque at the n^{th} joint can be expressed as:

$$\begin{aligned} \Delta f_n &= {}_{e}^{n}R \cdot \Delta F_e + m_n \cdot \Delta\dot{v}_n \\ \Delta n_n &= {}_{e}^{n}R \cdot \Delta N_e + \Delta n_{cn} + r_{cn} \times \Delta f_{cn} + {}^{n}p_e \times {}_{e}^{n}R \cdot \Delta F_e \end{aligned} \tag{8}$$

Wherein, ΔF_e and ΔN_e means the deviation of the external force and torque. If the external force is constant, then $\Delta F_e = 0$, $\Delta N_e = 0$. Then for an arbitrary joint i of space manipulator, the deviations of force and torque can be expressed:

$$\Delta f_i = \begin{cases} {}_{i+1}^{i}R \cdot \Delta f_{i+1} & i \in [1, k] \\ {}_{i+1}^{i}R \cdot \Delta f_{i+1} + \Delta f_{ci} & i \in [k+1, n] \end{cases} \tag{9}$$

$$\Delta n_i = \begin{cases} {}_{i+1}^{i}R \cdot \Delta n_{i+1} + {}^{i}p_{i+1} \times {}_{i+1}^{i}R \cdot \Delta f_{i+1} & i \in [1, k-1] \\ {}_{i+1}^{i}R \cdot \Delta n_{i+1} + \Delta n_{ci} + r_{ci} \times \Delta f_{ci} + {}^{i}p_{i+1} \times {}_{i+1}^{i}R \cdot \Delta f_{i+1} & i \in [k, n] \end{cases} \tag{10}$$

During Equation (9) and (10), when $i = n$, $\Delta f_{i+1} = \Delta F_e$, $\Delta n_{i+1} = \Delta N_e$. In conclusion, the vector of joint impact torque is derived:

$$\Delta\boldsymbol{\tau} = \begin{bmatrix} \Delta\boldsymbol{n}_1 & \dots & \Delta\boldsymbol{n}_n \end{bmatrix}^{\mathrm{T}} \tag{11}$$

And the z-component can be obtained as:

$$\Delta\tilde{\boldsymbol{\tau}} = \begin{bmatrix} \Delta\boldsymbol{n}_1 \cdot \boldsymbol{z} & \dots & \Delta\boldsymbol{n}_n \cdot \boldsymbol{z} \end{bmatrix}^{\mathrm{T}} \tag{12}$$

The x and y component can be obtained in a similar way. So far, the model of joint impact torque is established. The x, y component of impact torque can be offset by structure of space manipulator, while the z-component can be reduced by adjusting the output torque of joints. The paper aims at suppressing the z-component of joint impact torque, which can significantly reduce the damage to healthy joint when joint-locked failure occurs.

4. Suppression Control Method for Joint Impact Torque

Aiming at guaranteeing external force requirement and reducing the joint impact torque, a control method is proposed based on global torque compensation during the entire operation. The global compensation means to introduce joint torque compensation both before and after joint-locked failure. In this way, compensation before failure occurrence can improve the ability of failure tolerance, which also acts as feed-forward compensation for sudden failure to achieve better suppression performance. And compensation after joint failure is applied to smooth the joint torque. As a result, the external force is guaranteed and joint impact torque reduction is achieved simultaneously. In order to derive the control method, boundary conditions considering task constraints and parameters threshold should be analyzed first.

4.1. Boundary Conditions for Suppression Control

During space manipulator operations, the requirement of external force at the end-effector should be guaranteed, namely the actual value should be consistent with the desired value.

$$\boldsymbol{h}(t) = \boldsymbol{F}_e^a(t) - \boldsymbol{F}_e^d(t) \tag{13}$$

Wherein, $\boldsymbol{F}_e^a$ represents the actual value of external force at the end-effector, while $\boldsymbol{F}_e^d$ represents the desired value. Besides, the joint torque should not exceed the rated torque during operation, namely

$$\boldsymbol{g}_j(t) = \boldsymbol{\tau}_j(t) - \boldsymbol{\tau}_j^r \tag{14}$$

The subscript of j represents the joint number, $j = 1, \ldots, n$. And $\boldsymbol{\tau}_j^r$ represents the rated torque of the j^{th} joint.

4.2. Global Torque Compensation

Generally, the manipulability $w = \sqrt{\det\left(\boldsymbol{J} \cdot \boldsymbol{J}^{\mathrm{T}}\right)}$ is used to express the dexterity of space manipulator, which is often applied in reducing the velocity jump caused by joint failure [11]. However, the impact torque is related to the space manipulator dynamics. Taking this into account, the inertia matrix $\boldsymbol{M}$ which reflects the variation in configuration, load and joint status of space manipulator is introduced to construct the dynamics manipulability [14].

$$w_D = \sqrt{\det\left[\left(\boldsymbol{J} \cdot \boldsymbol{M}^{-1}\right)\left(\boldsymbol{J} \cdot \boldsymbol{M}^{-1}\right)^{\mathrm{T}}\right]} = \sqrt{\det\left[\boldsymbol{J}\left(\boldsymbol{M}^T\boldsymbol{M}\right)^{-1}\boldsymbol{J}^{\mathrm{T}}\right]} \tag{15}$$

According to the duality principle, the relationship between external force at the end-effector and joint driving torque can be expressed as $\boldsymbol{\tau} = \boldsymbol{J}^{\mathrm{T}}\boldsymbol{F}_e$, which can be transformed as $\boldsymbol{F}_e = \left(\boldsymbol{J}^{\mathrm{T}}\right)^{-1}\boldsymbol{\tau}$. Define $\tilde{\boldsymbol{J}} = \left(\boldsymbol{J}^{\mathrm{T}}\right)^{-1}$, the joint torque can be expressed as $\boldsymbol{\tau} = \tilde{\boldsymbol{J}}^{-1}\boldsymbol{F}_e$. Then taking the gradient of dynamics manipulability as torque compensation weight, the compensation function is constructed with the orthogonal basis of Jacobian null space.

$$\boldsymbol{U}(t) = k_d \cdot \left(\boldsymbol{I} - \left(\tilde{\boldsymbol{J}}\left(\boldsymbol{q}(t)\right) \right)^{\dagger} \tilde{\boldsymbol{J}}\left(\boldsymbol{q}(t)\right) \right) \cdot \nabla \boldsymbol{w}_D(\boldsymbol{q}(t)) \tag{16}$$

The torque compensation function takes operation time t as independent variables. In Equation (16), $\boldsymbol{q}(t)$ represents the joint angle at time t. Based on the torque compensation function, the compensated joint torque is expressed as:

$$\tilde{\boldsymbol{\tau}}(t) = \tilde{\boldsymbol{J}}^{-1}(\boldsymbol{q}(t)) \cdot \boldsymbol{F_e} + \boldsymbol{U}(t) \tag{17}$$

And the joint impact torque after compensation can be expressed as:

$$\Delta\tilde{\boldsymbol{\tau}} = \tilde{\boldsymbol{\tau}}(t_f + \Delta t) - \tilde{\boldsymbol{\tau}}(t_f) \tag{18}$$

In Equation (16), $\boldsymbol{U}(t)$ changes with the coefficient $\boldsymbol{k}_d$, then has further effect on $\Delta\tilde{\boldsymbol{\tau}}$. If the coefficient is constant and the objective function is established as the norm of vector $\Delta\tilde{\boldsymbol{\tau}}$, it may cause when the objective function is minimal, impact torque of some joints become larger [11]. In order to avoid this problem, the coefficient is represented as diagonal matrix, during which joint i has its unique compensation element k_{di}.

$$\boldsymbol{k}_d = diag\left[k_{d1}, \ldots k_{di}, \ldots k_{dn}\right] \tag{19}$$

Then Equation (16) can be transformed into:

$$\boldsymbol{U}(t) = \left(\boldsymbol{I} - \left(\tilde{\boldsymbol{J}}\left(\boldsymbol{q}(t)\right) \right)^{\dagger} \tilde{\boldsymbol{J}}\left(\boldsymbol{q}(t)\right) \right) \cdot \boldsymbol{k}_d \cdot \nabla \boldsymbol{w}_D(\boldsymbol{q}(t)) \tag{20}$$

Aiming at minimizing the impact torque of each joint, the objective function can be expressed as a group of functions $\left\{ \boldsymbol{f} \right\}_k$, $k = 1, \ldots, n$. Then the mathematical expression of the suppression control method can be derived.

$$\begin{aligned} &\min \quad \left\{ \boldsymbol{f} \right\}_k = \left| \Delta\tilde{\tau}_k \right|, k = 1, \ldots, n \\ &\text{s.t.} \quad \boldsymbol{g}_i(t) \le 0 \\ &\qquad \boldsymbol{h}(t) = 0, i = 1, \ldots, n \end{aligned} \tag{21}$$

Wherein $\Delta\tilde{\tau}_k$ represents the k^{th} element of vector $\Delta\tilde{\boldsymbol{\tau}}$. In a word, the suppression control method for joint impact torque can be explained as: find a proper coefficient $\boldsymbol{k}_d$ to minimize the objective function on the premise of guaranteeing the boundary conditions.

4.3. Calculation Process for the Suppression Control Method

In order to calculate Equation (21), the gradient of dynamics manipulability should be firstly calculated, which can be represented as:

$$\nabla \boldsymbol{w}_D\left(\boldsymbol{q}\right) = \frac{\partial w_D}{\partial \boldsymbol{q}} = \left(\frac{\partial w_D}{\partial q_1}, \ldots, \frac{\partial w_D}{\partial q_i}, \ldots \frac{\partial w_D}{\partial q_n} \right)^{\mathrm{T}}, i = 1, \ldots, n \tag{22}$$

The partial deviation of dynamics manipulability with respect to each joint angle can be expressed as:

$$\frac{\partial w_D}{\partial q_i} = \frac{\partial \sqrt{\det\left(\boldsymbol{J}\left(\boldsymbol{M}^{\mathrm{T}} \boldsymbol{M} \right)^{-1} \boldsymbol{J}^{\mathrm{T}} \right)}}{\partial q_i} = \frac{\partial \left(\det\left(\boldsymbol{J}\left(\boldsymbol{M}^{-1} \left(\boldsymbol{M}^{-1} \right)^{\mathrm{T}} \right) \boldsymbol{J}^{\mathrm{T}} \right) \right) / \partial q_i}{2 w_D} \tag{23}$$

Define $\boldsymbol{H}(\boldsymbol{q}) = \boldsymbol{J}(\boldsymbol{q})\boldsymbol{M}(\boldsymbol{q})^{-1}$, Equation(23) can be transferred as:

$$\frac{\partial w_D}{\partial q_i} = \frac{\partial \sqrt{\det\left(\boldsymbol{H}\boldsymbol{H}^{\mathrm{T}} \right)}}{\partial q_i} = \frac{\partial \left(\det\left(\boldsymbol{H}\boldsymbol{H}^{\mathrm{T}} \right) \right) / \partial q_i}{2 w_D} \tag{24}$$

During which, it has

$$\frac{\partial\left(\det\left(\boldsymbol{H}\boldsymbol{H}^{\mathrm{T}}\right)\right)}{\partial q_i}=\sum_{j=1}^{n}\det\left(\begin{array}{cccccc}\left(\boldsymbol{H}\boldsymbol{H}^{\mathrm{T}}\right)_1 & \left(\boldsymbol{H}\boldsymbol{H}^{\mathrm{T}}\right)_2 & \cdots & \dfrac{\partial\left(\boldsymbol{H}\boldsymbol{H}^{\mathrm{T}}\right)_j}{\partial q_i} & \cdots & \left(\boldsymbol{H}\boldsymbol{H}^{\mathrm{T}}\right)_n\end{array}\right) \tag{25}$$

Wherein, $\dfrac{\partial\left(\boldsymbol{H}\boldsymbol{H}^{\mathrm{T}}\right)_j}{\partial q_i}=\left(\dfrac{\partial\left(\boldsymbol{H}\boldsymbol{H}^{\mathrm{T}}\right)}{\partial q_i}\right)_j$, namely the j^{th} row of $\dfrac{\partial\left(\boldsymbol{H}\boldsymbol{H}^{\mathrm{T}}\right)}{\partial q_i}$. Then:

$$\frac{\partial\left(\boldsymbol{H}\boldsymbol{H}^{\mathrm{T}}\right)}{\partial q_i}=\frac{\partial\boldsymbol{H}}{\partial q_i}\boldsymbol{H}^{\mathrm{T}}+\boldsymbol{H}\left(\frac{\partial\boldsymbol{H}}{\partial q_i}\right)^{\mathrm{T}} \tag{26}$$

In Equation(26), $\dfrac{\partial\boldsymbol{H}}{\partial q_i}$ can be calculated as:

$$\frac{\partial\boldsymbol{H}}{\partial q_i}=\frac{\partial(\boldsymbol{J}\boldsymbol{M}^{-1})}{\partial q_i}=\frac{\partial\boldsymbol{J}}{\partial q_i}\boldsymbol{M}^{-1}+\boldsymbol{J}\frac{\partial\boldsymbol{M}^{-1}}{\partial q_i} \tag{27}$$

Then by giving the value of $\partial\boldsymbol{J}/\partial q_i$ and $\partial\boldsymbol{M}^{-1}/\partial q_i$, the gradient of dynamics manipulability at each time of operation can be calculated. After joint k fails, $\partial w_D/\partial q_k=0$, which means no compensation is applied on the failure joint after joint failure.

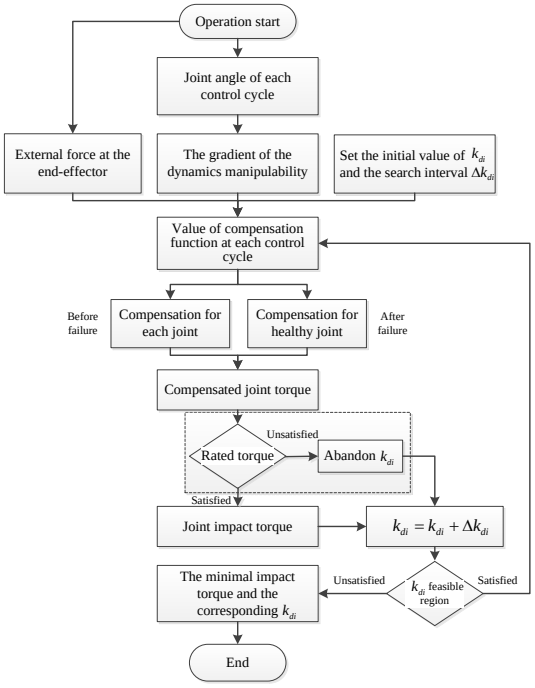

Figure 2. Calculation Process for Suppression Control Method

Besides, in order to obtain the compensation torque at each time, $\boldsymbol{k}_d$ should be determined. So the initial value of k_{di} and the interval Δk_{di} should be set, and search algorithm is carried out to search for the optimal k_{di}. k_{di} should be searched in a feasible region $[k_{di}^{\mathrm{down}}, k_{di}^{\mathrm{up}}]$, whose boundary should guarantee:

$$k_{di}^{\text{up}} = \min_{t\in(t_0,t_e)} \boldsymbol{U}^{-1}\left(\boldsymbol{\tau}_i^r - \boldsymbol{J}^{\mathrm{T}}\boldsymbol{F}_e\right)$$
$$k_{di}^{\text{down}} = \max_{t\in(t_0,t_e)} \boldsymbol{U}^{-1}\left(-\boldsymbol{\tau}_i^r - \boldsymbol{J}^{\mathrm{T}}\boldsymbol{F}_e\right) \quad (28)$$

Wherein, t_0 and t_e represent the initial and end time of operation. As a result, the optimal $\boldsymbol{k}_d$ and the corresponding joint torque can be obtained. The calculation process is shown in figure 2. In this section, the suppression control method is detailed discussed from boundary conditions, global compensation function and calculation process. Self-motion of space manipulator is applied to achieve torque adjustment by using gradient of dynamics manipulability as compensation weight. Coefficient $\boldsymbol{k}_d$ is treated as decision variable to achieve impact torque optimization. As a result, suppression for joint impact torque is achieved by global torque compensation during the entire operation.

5. Simulation Experiments

5.1. Parameters of Space Manipulator

Simulation experiments are carried out on a 7 degree of freedom (DOF) space manipulator whose configuration is similar to SSRMS [1]. The kinematics and dynamics parameters are list in Table 1, and the joint coordinates are shown in Figure 3. This paper aims at suppressing the impact torque caused by joint-locked failure when external force acts on the end-effector. In order to deal with the diversity of space manipulator operations on orbit, the external force is divided into constant force and variable force. Path planning as typical space manipulator operation is applied to analyze the impact torque suppression in the paper. The planning time is 20s and the joint-locked failure is assumed to occur in joint 2.

Table 1. Kinematics and Dynamics Parameters of Space Manipulator

	Joint 1	Joint 2	Joint 3	Joint 4	Joint 5	Joint 6	Joint 7
$\theta_i(°)$	0	90	0	0	0	-90	0
d_i(m)	0.6	0.5	0.5	0.5	0.5	0.5	0.6
a_{i-1}(m)	0	0	5	5	0	0	0
$\alpha_{i-1}(°)$	90	-90	0	0	90	-90	0
Mass (kg)	42.5	42.5	70	70	42.5	42.5	42.5
centroid position p_x(m)	0	0	2.5	2.5	0	0	0
centroid position p_y(m)	0.25	0.25	0	0	0	0	0
centroid position p_z(m)	0	0	0	0	-0.25	-0.25	-0.3
Inertia I_{xx}($\mathrm{kg}\cdot\mathrm{m}^2$)	0.8854	0.8854	0.0875	0.0875	0.8854	0.8854	1.2750
Inertia I_{yy}($\mathrm{kg}\cdot\mathrm{m}^2$)	0.0531	0.0531	145.8333	145.8333	0.8854	0.8854	1.2750
Inertia I_{zz}($\mathrm{kg}\cdot\mathrm{m}^2$)	0.8854	0.8854	145.8333	145.8333	0.0531	0.0531	0.0531

Note: Product of inertia for each joint equals to 0.

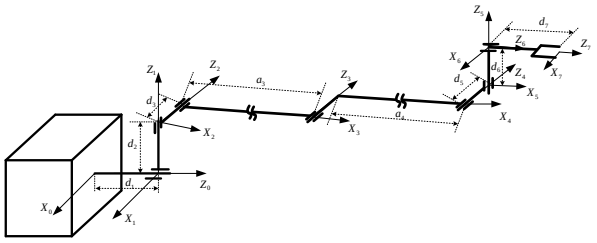

Figure 3. The Joint Coordinates of Space Manipulator

5.2. Impact Torque Suppression under Constant External Force

Set the external force acted on the end-effector as $\boldsymbol{F}_e = \begin{bmatrix} 20 & 20 & 20 \end{bmatrix}^{\mathrm{T}}$ (N) during path planning. According to the proposed control method for joint impact torque suppression, set the initial value of each element of the diagonal matrix as 0, and the search interval is set as $\Delta k_{di} = \pm 1e^7$. Namely the coefficient is searched from positive and negative compensation, respectively. Then when joint fails at 10s, the optimal diagonal matrix coefficient is obtained.

$$\boldsymbol{k}_d = diag\begin{bmatrix} -10.0 & -9.9 & -10.1 & -10.7 & -8.5 & -12.4 & 0 \end{bmatrix} \cdot e^7 \tag{29}$$

The torques of joint 1 and 3 after suppressing control are shown in Figure 4. In the figure, large deviations are brought in joint torque when joint-locked failure occurs. After suppression control is applied, the impact torques are significantly reduced. The joint torques variation of other joints are list in Table 2. It can be found that the impact torques caused by joint-locked failure are larger in joints 1-3 and smaller in joints 4-6. Anyway, the impact torque in each joint can be reduced with the proposed suppression method in the paper, and the suppression ratio is over 95%. Besides, since no impact torque is brought in joint 7 when joint fails, suppression for torque of joint 7 is not needed. The corresponding coefficient of joint 7 is set as 0.

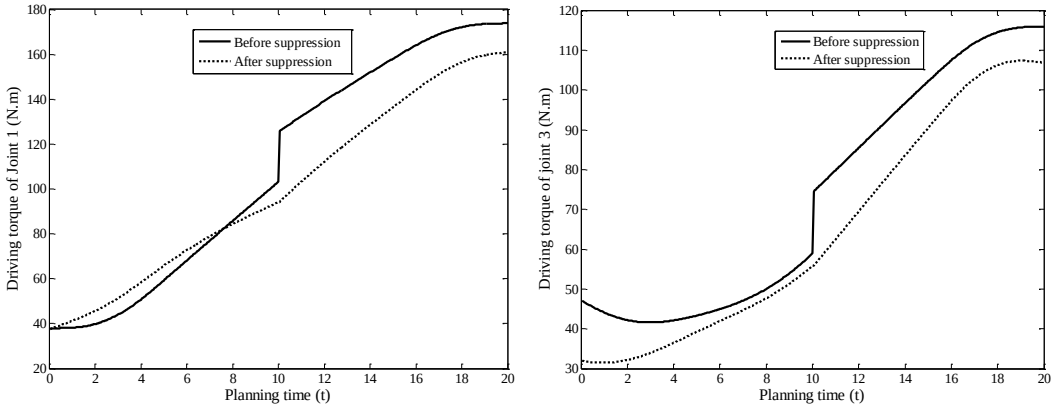

(a) Joint 1 (b) Joint 3

Figure 4. Suppression for Joint Impact Torque under Constant External Force

In Table 2, the joint torque variation when joint failure occurs at 3s and 18s are given out. Since the path is planned according to trapezoidal planning with parabola transition, it is consist of acceleration phase, uniform phase and decelerating phase, which are represented by 3s, 10s and 18s respectively. It can be found that the suppression performances are similar in acceleration phase (3s) and uniform phase

(10s), whose suppression ratios are both over 90% for each joint. While the suppression ratio is smaller at 18s, which is about 50% averagely.

Table 2. Comparison of Joint Impact Torque before and After Suppression

Joint number	Joint-locked failure at 10s		Joint-locked failure at 3s		Joint-locked failure at 18s	
	Impact torque before suppression $(\mathrm{N}\cdot\mathrm{m})$	Impact torque after suppression $(\mathrm{N}\cdot\mathrm{m})$	Impact torque before suppression $(\mathrm{N}\cdot\mathrm{m})$	Impact torque after suppression $(\mathrm{N}\cdot\mathrm{m})$	Impact torque before suppression $(\mathrm{N}\cdot\mathrm{m})$	Impact torque after suppression $(\mathrm{N}\cdot\mathrm{m})$
1	30.18	0.1472	46.56	0.045	6.90	3.93
2	66.72	0.1368	30.31	0.020	46.00	23.68
3	20.48	0.1091	6.42	0.040	8.62	4.58
4	1.24	0.0058	0.42	$1.20e^{-4}$	0.36	0.013
5	0.67	$8.591e^{-4}$	0.17	0.0026	0.069	0.069
6	3.04	0.0091	1.54	0.0034	0.58	$5.3e^{-4}$
7	0	0	0	0	0	0

In conclusion, the feasibility of the proposed suppression control method is verified no matter when joint-locked failure occurs in space manipulator operation with constant external force acting on the end-effector. And the joint impact torque can be suppressed to minimal in numerical with the proposed method.

5.3. Impact Torque Suppression Considering Rated Torque

From Table 2, the impact torques in joints 4-6 are not too large after joint-locked failure occurs, and the torques of joints 4-6 before and after impact torque suppression can be obtained in Figure 5.

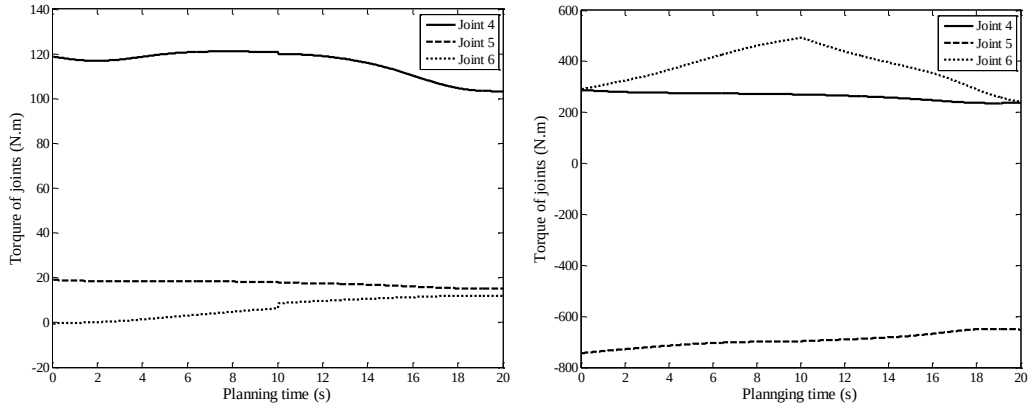

(a) Joint torque before suppression (b) Joint torque after suppression

Figure 5. Torques of Joints 4-6 before and After Impact Torque Suppression

It can be found that in joint 5 and 6, large torque compensation are introduced to suppress the impact torque. Although the impact torque can be optimized in numerical, the compensated torques are too large, which may exceed the limitation of joint torque. Then considering the limitation of joint rated torque, the suppression performance will be changed, which will be detailed discussed in this section.

Define the rated torque of space manipulator as $\boldsymbol{\tau}^r = [\tau_1^r, \ldots, \tau_i^r, \ldots, \tau_n^r]^{\mathrm{T}}$, which is taken as the boundary of joint torque. For joint i, part of the joint torque $\boldsymbol{\tau}_i^v$ is used to drive joint moving, the other part $\boldsymbol{\tau}_i^e$ is used to achieve force equilibrium when external force acts at the end-effector. And it guarantees $\boldsymbol{\tau}_i^e = \boldsymbol{\tau}_i^r - \boldsymbol{\tau}_i^v$. $\boldsymbol{\tau}_i^v$ is influenced by joint velocity,

and changes with operation time. Once $\boldsymbol{\tau}_i^r$ is determined, $\boldsymbol{\tau}_i^e$ can be correspondingly calculated. Assume the rated torque of each joint is equivalent as $\boldsymbol{\tau}_i^r = 300\mathrm{N}\cdot\mathrm{m}$. Then the optimal coefficient of compensation function is corrected considering the constraints of rated torque.

$$\boldsymbol{k}_d = diag\left[-10.0 \quad -9.9 \quad -10.1 \quad -6.7 \quad -2.9 \quad -5.2 \quad 0\right]\cdot e^7 \tag{30}$$

The torques of joints 4-6 after impact torque suppression considering rated torque are obtained in Figure 6. $\boldsymbol{\tau}_i^v$ is calculated according to Newton-Euler dynamics, then the average value of $\boldsymbol{\tau}_i^e$ can be obtained, $\overline{\boldsymbol{\tau}}_i^e = 254.18\mathrm{N.m}$. From the figure, the compensated torques of joints 4-6 are limited to $\overline{\boldsymbol{\tau}}_i^e$. And compared with the situation when rated torque is not considered, the compensated torques for joints 4-6 decrease 21.58%、67.57%、56.84%, respectively.

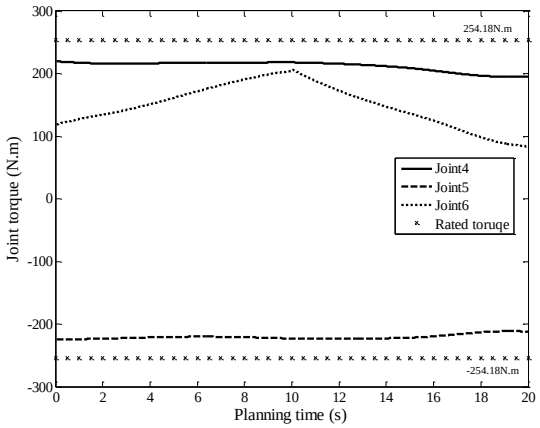

Figure 6. Joint Torque Considering the Constraints of Rated Torque

Table 3. Suppression for Impact Torque of Joints 4-6 Considering Rated Torque

Joint number	Joint 4	Joint 5	Joint 6
Impact torque before suppression $(\mathrm{N}\cdot\mathrm{m})$	1.24	0.67	3.04
Impact torque after suppression $(\mathrm{N}\cdot\mathrm{m})$	0.0058	$8.591\mathrm{e}^{-4}$	0.0091
Suppression rate $(\%)$	99.53	99.87	99.70
Suppression considering rated torque $(\mathrm{N}\cdot\mathrm{m})$	0.2684	0.5063	1.4558
Suppression rate $(\%)$	78.35	24.43	52.11

Following the decrease in compensated torque, the suppression rate for impact torque of joints 4-6 decrease 21.18%、75.44%、47.59% correspondingly, which is shown in Table 3. Under the limitation of rated torque, the reduction for joint impact torque can also be achieved with the proposed suppression control method. Although the suppression ratio decreases, the suppressed joint torque is acceptable in application.

5.4. Suppression for Joint Impact Torque under Variable External Force

Considering the variety of on-orbit operations, the external force acts on the end-effector of space manipulator is different. During some operations, the external force is time-varying. In this section, the feasibility of the proposed suppression control method is analyzed with the external force in quadratic function form. Define the external force in the following form:

$$\boldsymbol{F}_e(t) = 0.2t^2 + 4t \tag{31}$$

Define the rated torque of each joint as $\boldsymbol{\tau}_i^r = 300\mathrm{N}\cdot\mathrm{m}$. Path planning is carried out and the optimal coefficient of compensation function when joint-locked failure occurs at 3s, 10s, and 18s in the operation are obtained in Table 4. Meanwhile, the joint impact torque is compared in Figure 7.

Table 4. The Optimal Coefficients for Suppression of Joint Impact Torque

Failure time	$k_{d1}(\cdot e^8)$	$k_{d2}(\cdot e^8)$	$k_{d3}(\cdot e^8)$	$k_{d4}(\cdot e^8)$	$k_{d5}(\cdot e^8)$	$k_{d6}(\cdot e^8)$	$k_{d7}(\cdot e^8)$
3s	-0.29	-0.27	-0.29	0.50	0	-0.36	0
10s	-0.90	-0.85	-0.90	-0.85	-1.20	-1.00	0
18s	-0.82	-1.16	-0.90	-0.52	0	-0.45	0

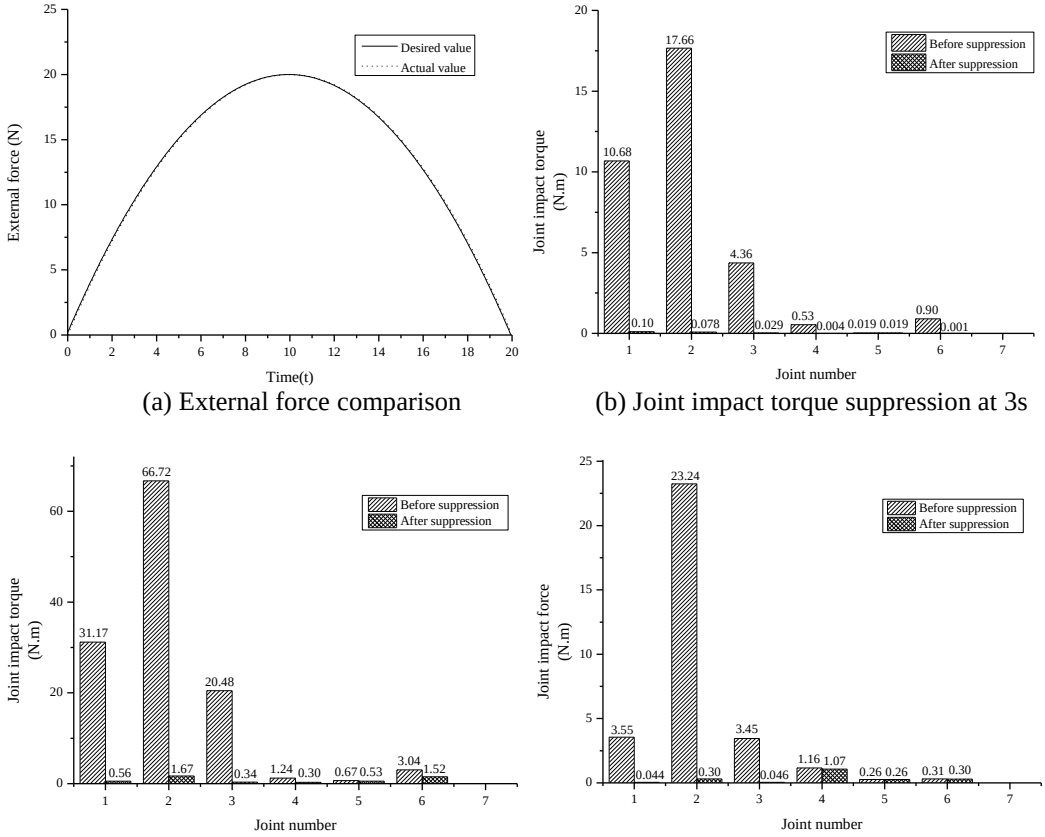

(a) External force comparison (b) Joint impact torque suppression at 3s

(c) Joint impact torque suppression at 10s (d) Joint impact torque suppression at 18s

Figure 7. Joint Impact Torque Comparison at Different Failure Time

From Figure 7(a), although the external force is variable force, it can be guaranteed when the joint impact torques are suppressed. In Figures 7(b)~(d), joint-locked failure which occurs earlier in the operation has better suppression performance. Since joints 1-3 are close to the base, their impact torques caused by joint-locked failure are obviously larger than joints 4-6. With the proposed suppression method, the impact torques of joints

1-3 can be significantly reduced. While for the impact torques of joints 4-6, the suppression performances are not so obvious by taking the rated torque into account. However, the impact torques of joints 4-6 can be reduced assuredly. And since the impact torques of joints 4-6 are small, they can be ignored in some conditions.

In conclusion, the control method proposed in the paper can achieve good performance in reducing joint impact torque, and guarantee the external force acting on the end-effector of space manipulator no matter constant force or variable force.

6. Conclusion

A control method of suppressing impact torque caused by joint-locked failure is proposed in the paper. With the method, the external force acting at the end-effector during on-orbit load operations of space manipulator can be guaranteed and the joint impact force can be significantly reduced simultaneously. Dynamics manipulability is introduced to represent the self-motion ability of space manipulator and global torque compensation is implemented during the entire operation. With the application of the method, it can be found:

(1) The method is adaptable for both constant external force and variable external force, and can achieve impact torque suppression for failure at arbitrary time in operation.

(2) When joint 2 fails, impact torques of joints 1-3 are larger and the suppression performance in joints 1-3 is better. Impact torques of joints 4-6 are smaller, and the suppression need larger joint torque compensation. Thus rated torque of each joint should be considered to make the torque compensation reasonable. And since impact torque of joints 4-6 are small, whether the impact torque need to be suppressed should be determined according to practical application.

(3) The proposed method can be applied for arbitrary joint-locked failure of serial manipulator and can be developed for multiple joints failure condition.

Acknowledgments

This work is supported by the National Natural Science Foundation of China (61403038), the National Key Basic Research Program of China (2013CB733000) and the National Natural Science Foundation of China (61175080).

References

[1] R. McGregor and L. Oshinowo, “Flight 6A: Deployment and Checkout of the Space Station Remote Manipulator System (SSRMS)”, Proceedings of the 6th International Symposium on Artificial Intelligence, Robotics and Automation in Space (i-SAIRAS), **(2001)**.

[2] Y. Kazuya, “Achievements in space robotics”, Robotics & Automation Magazine, IEEE, vol.16, no.4, **(2009)**, pp. 20-28.

[3] P. Putz, “Space robotics in Europe: A survey”, Robotics and Autonomous Systems, vol.23, no.1, **(1998)**, pp. 3-16.

[4] R. S. Jamisola, A. A. Maciejewski and R. G. Roberts, “Failure-tolerant path planning for kinematically redundant manipulators anticipating locked-joint failures”, Robotics, IEEE Transactions on, vol.22, no.4, **(2006)**, pp. 603-612.

[5] G. Ferretti and G. Magnani, “Zavala Rio A. Impact modeling and control for industrial manipulators”, Control Systems, IEEE, vol.18, no.4, **(1998)**, pp. 65-71.

[6] D-G Zhang and J Angeles, “Impact dynamics of flexible-joint robots”, Computers & Structures, vol.83, no.1, **(2005)**, pp. 25-33.

[7] D. N. Nenchev and Y. Kazuya, “Impact analysis and post-impact motion control issues of a free-floating Space robot subject to a force impulse”, Robotics and Automation, IEEE Transactions on, vol.15, no.3, **(1999)**, pp. 548-557.

[8] W. J. Chung, I. H. Kim and J. Joh, “Null-space dynamics-based control of redundant manipulators in reducing impact”, Control Engineering Practice, vol.5, no.9, **(1997)**, pp. 1273-1282.

[9] X. Wei, X. Rong and W. Jun, "Force/Torque-based Compliance Control for Humanoid Robot to Compensate the Landing Impact Force", proceedings of the Networking and Distributed Computing (ICNDC), **(2010)**, pp. 336-340.
[10] Z. Jing and F. Cheng, "On the joint velocity jump during fault tolerant operations for manipulators with multiple degrees of redundancy", Mechanism and Machine Theory, vol.44, no.6, **(2009)**, pp. 1201-1210.
[11] J. Qingxuan, L. Tong, C. Gang, S. Hanxu and Z. Jian,"Velocity jump reduction for manipulator with single joint failure", proceedings of the Multisensory Fusion and Information Integration for Intelligent Systems (MFI), 2014 International Conference on, **(2014)**, pp. 1-6.
[12] H. Abdi and S. Nahavandi, "Fault tolerance force for redundant manipulators", proceedings of the Advanced Computer Control (ICACC), 2010 2nd International Conference on, **(2010)**, pp. 612-617.
[13] H. Abdi, S. Nahavandi and M. T. Masouleh, "Minimal force jump within human and assistive robot cooperation", proceedings of the Intelligent Robots and Systems (IROS), 2010 IEEE/RSJ International Conference on, **(2010)**, pp. 2651-2656.
[14] S. Patel and T. Sobh, "Manipulator Performance Measures - A Comprehensive Literature Survey", Journal of Intelligent & Robotic Systems, vol.77, no.3, **(2015)**, pp. 547-570.

Authors

Tong Li, he received his B.S. degree of Engineering Mechanics in 2010 from Beijing University of Aeronautics and Astronautics, Beijing, China. And he is currently pursuing the M.S. degree of Mechanical and Electronic Engineering from Beijing University of Posts and Telecommunications, Beijing, China. His research interests include advanced robot technology, fault-tolerant control and trajectory optimization.

Qingxuan Jia, he is a Professor in School of Automation in Beijing University of Posts and Telecommunications, Beijing, China. He received his B.S. degree in Shandong University of Technology in 1982, and received his Ph.D. and M.S. degrees in Beijing University of Aeronautics and Astronautics in 1991 and 2005, respectively. His research interests are basic theory and application of robotics, space manipulator control and virtual reality technology.

